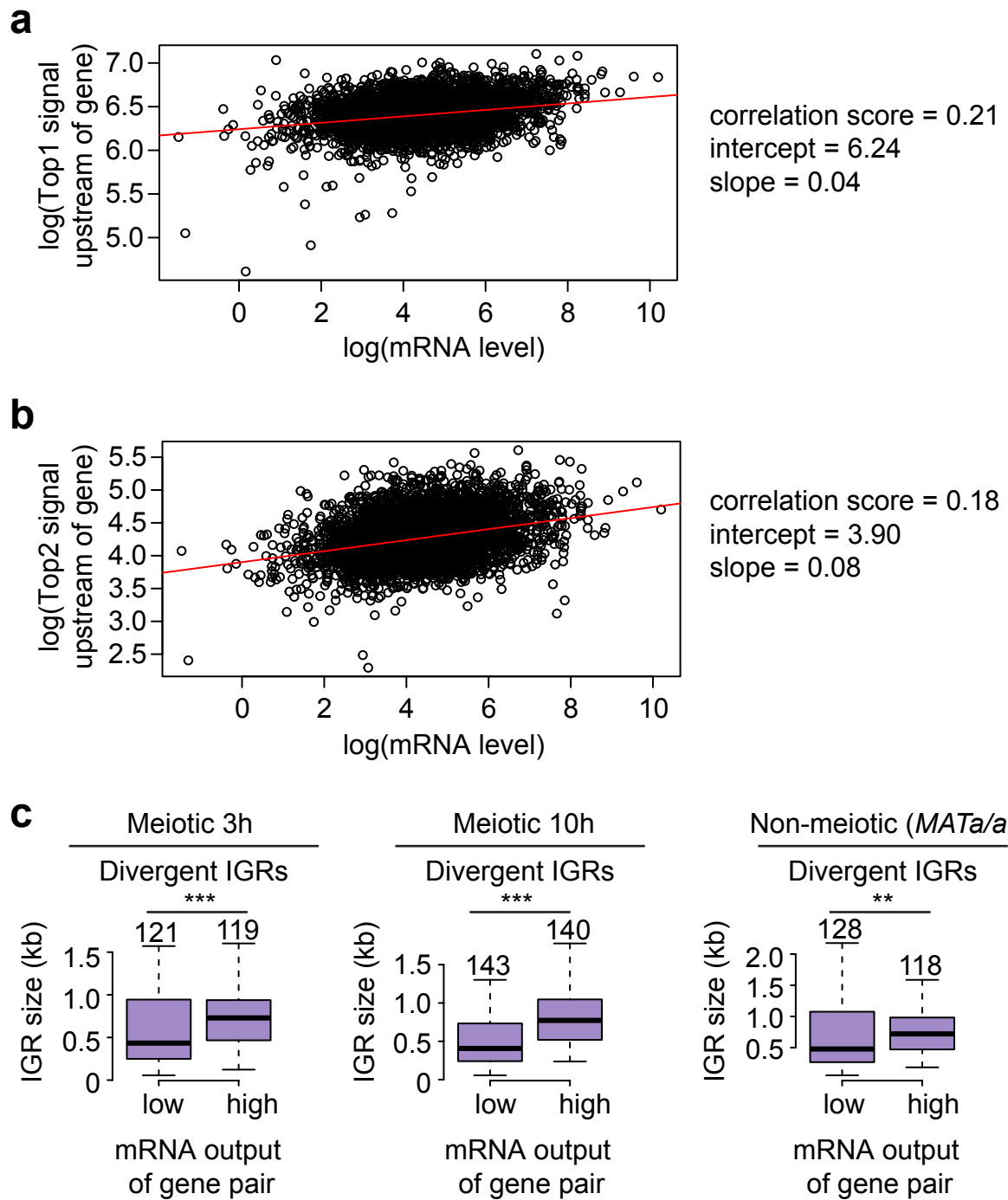


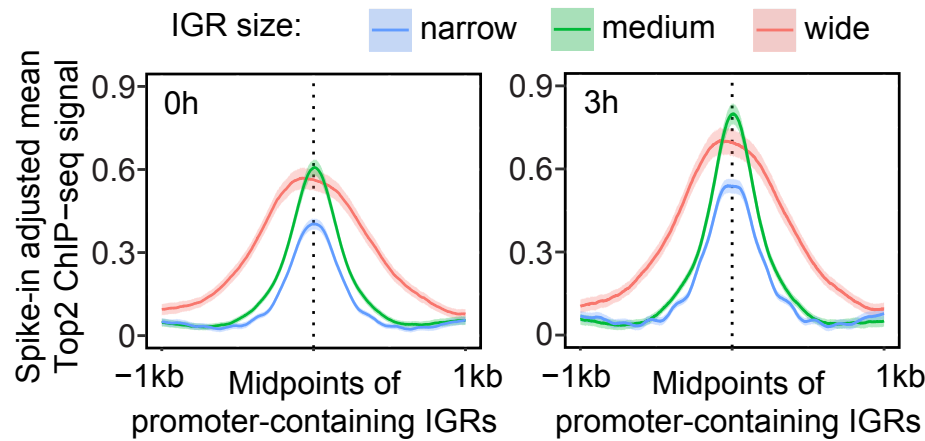
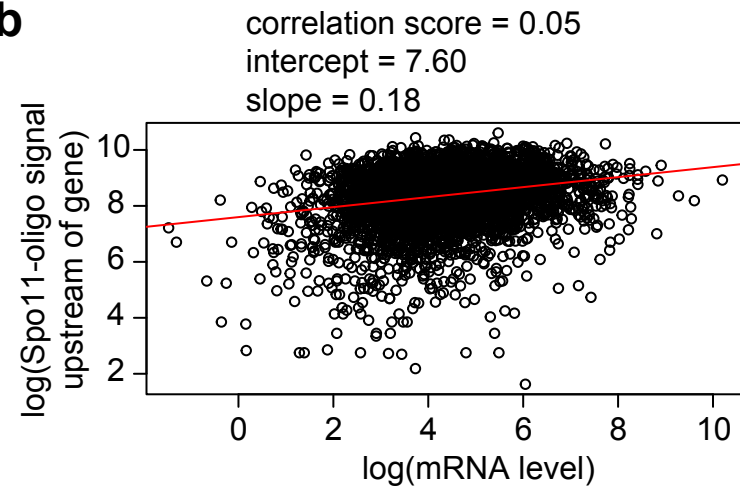
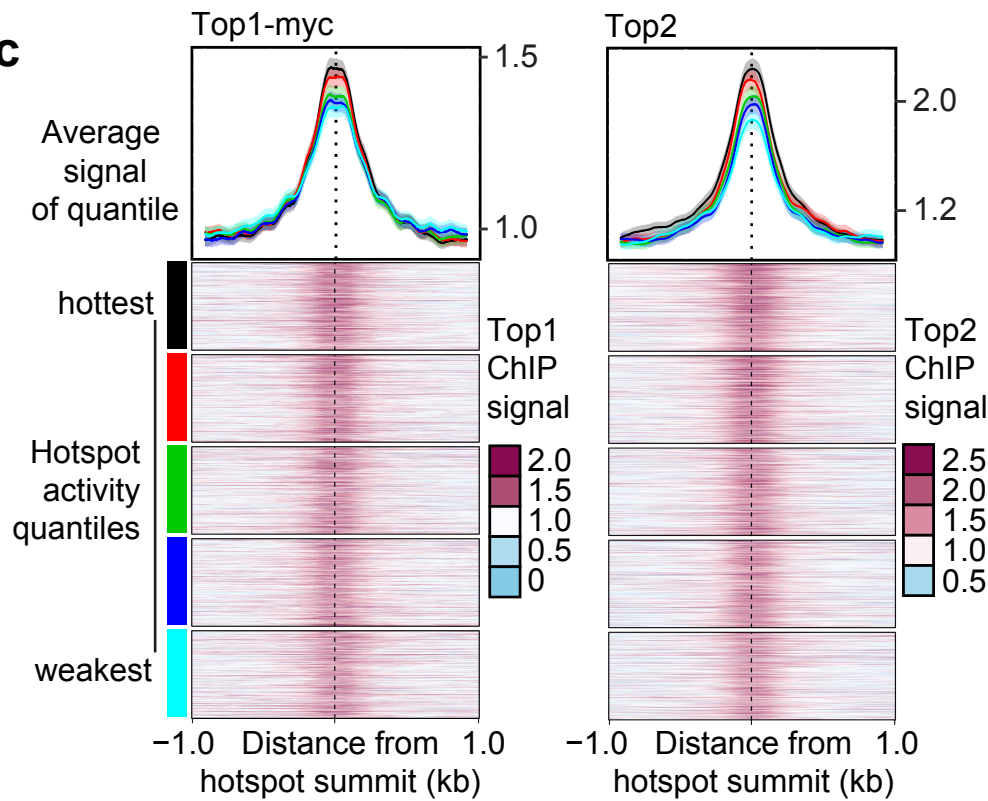
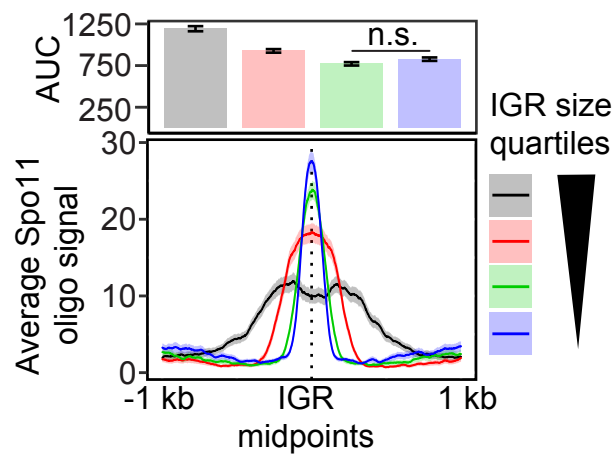
Supplemental Figure 1. Topoisomerases are abundant on chromosomes throughout meiotic prophase.

(a-b) Immunofluorescence staining of chromosome spreads throughout meiotic prophase. **(a)** Top1-13myc nuclei and wild-type no-tag control nuclei stained for the myc epitope, Zip1, and DAPI. White arrowhead marks the nucleolus. Scale bars are 5 μ m. **(b)** Wild-type nuclei stained for Top2, Zip1, and DAPI. Scale bars are 5 μ m. **(c)** Scatterplot showing the correlation between Top1-myc and Top2 ChIP-seq signal across the genome (correlation = 0.76). **(d)** Top1-13myc localization centered at the midpoints of IGRs, parsed into divergent, tandem, and convergent regions. The 95% confidence interval is shown for average lines.



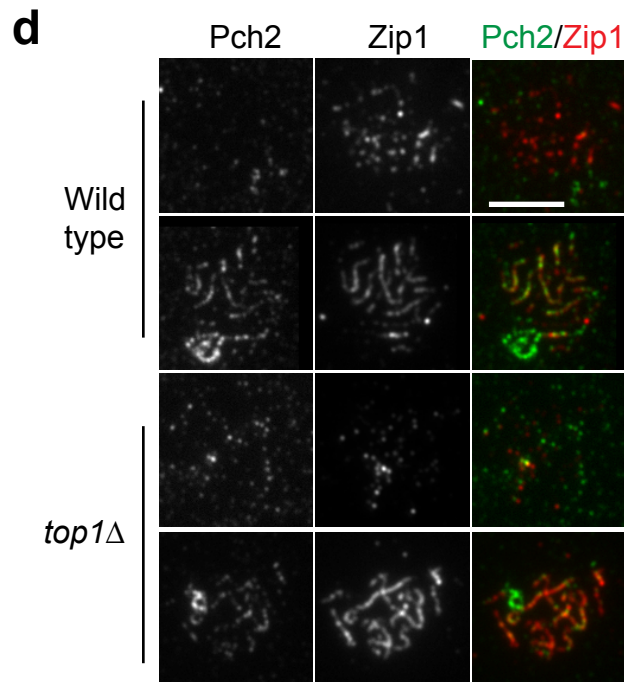
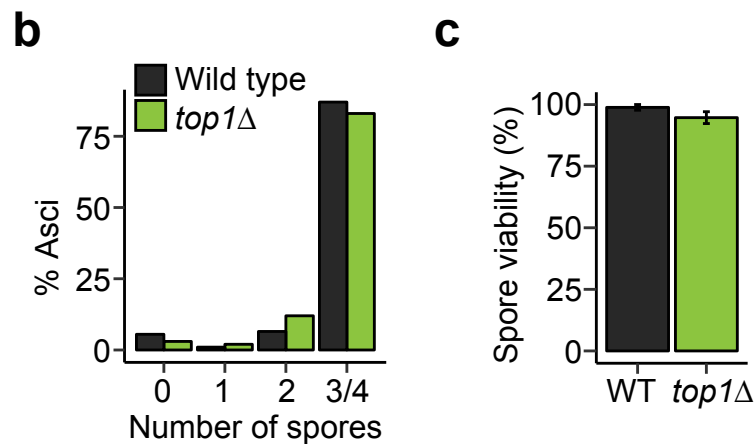
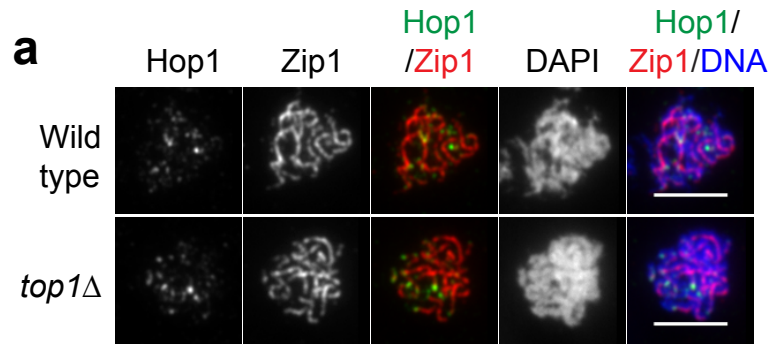
Supplemental Figure 2. Transcription is most active in genes sharing wide divergent promoter regions during starvation.

(a-b) Scatterplot comparing the relationship between mRNA level and Top1-13myc (a) and Top2 (b) signal. The values are in logarithmic scale. The red line shows the linear regression. Correlation score, intercept, and slope are noted. **(c)** Box plots showing the size distribution of divergent regions for highly and lowly transcribed gene pairs during meiosis at 3h and 10h and in non-meiotic *MATa/a* cells in sporulation medium (Cheng et al, 2018). The number of gene pairs is noted above the respective box. *** $P < 0.00001$, ** $P < 0.01$, Mann-Whitney-Wilcoxon test.

a**b****c****d**

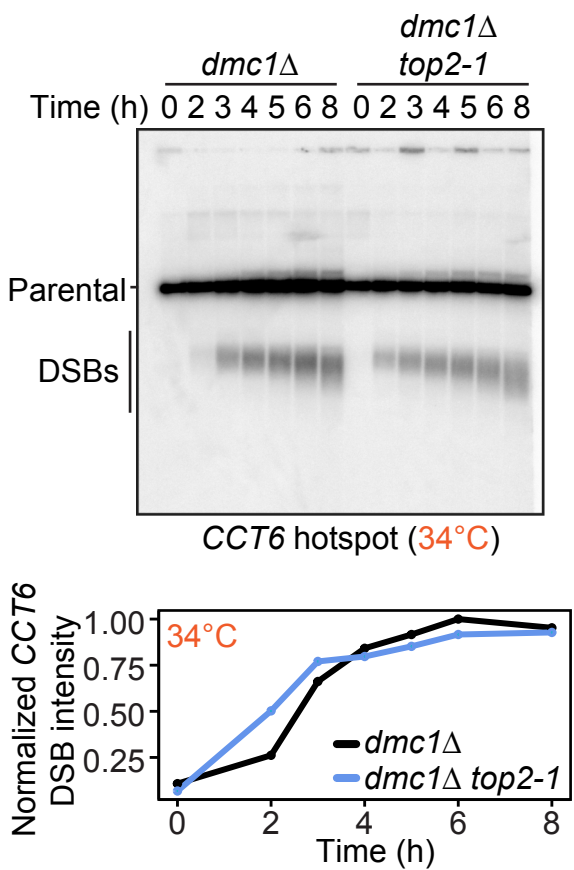
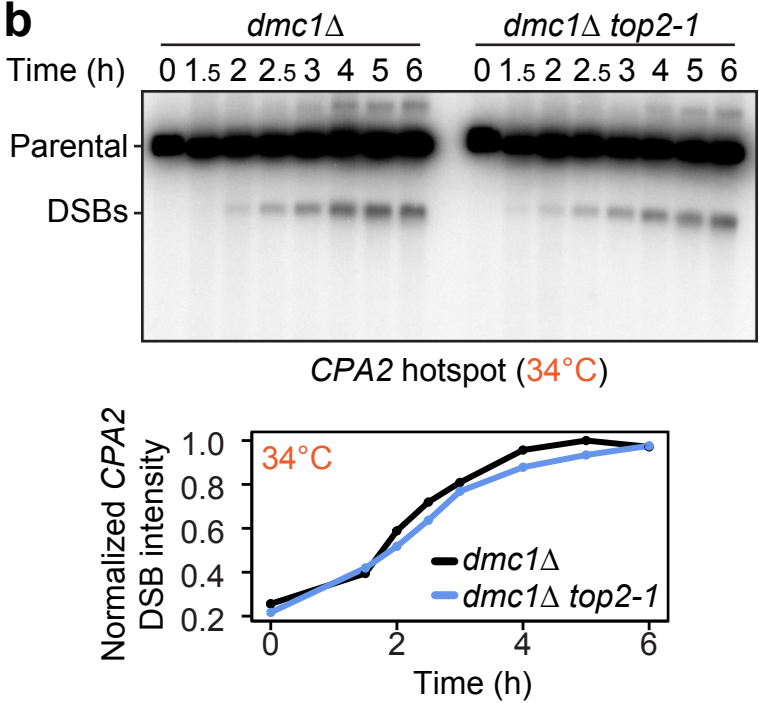
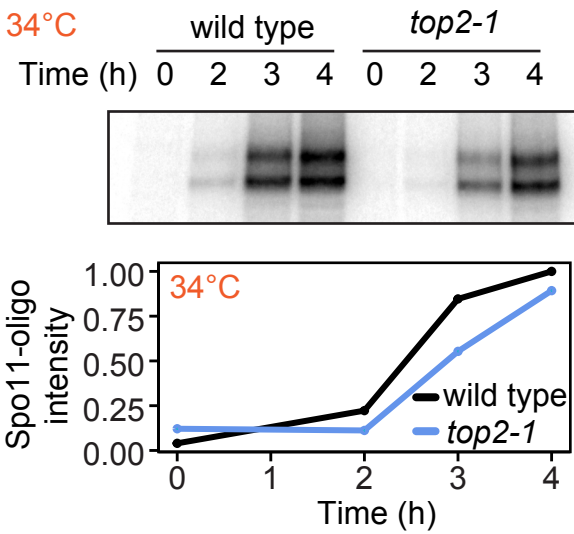
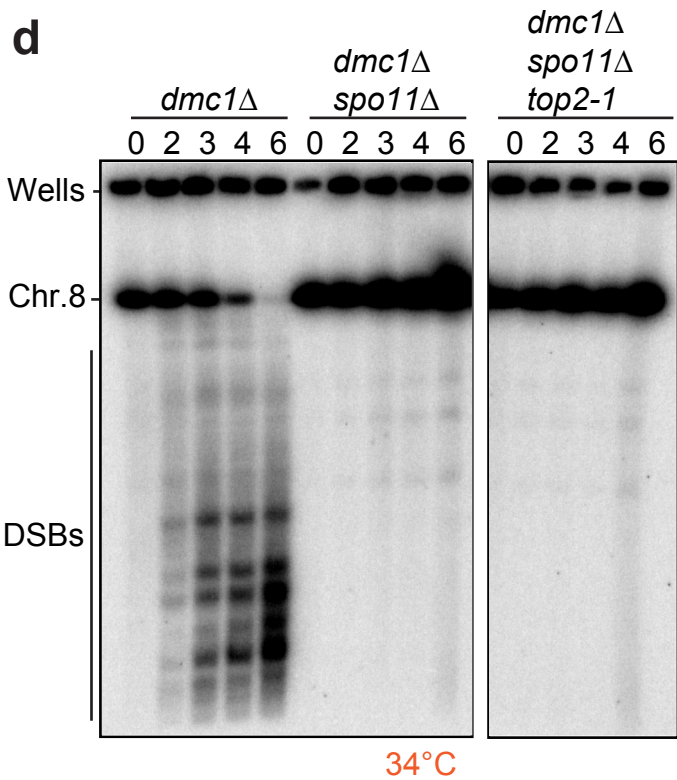
Supplemental Figure 3. Top2 abundance on chromosomes increases during meiosis.

(a) Top2 binding in promoters parsed by size of the promoter-containing IGR on pre-meiotic or meiotic chromosomes using quantitative SNP-ChIP normalization. Quantile ranges are <338 bp (narrow, blue), 338-625 bp (medium, green), and >625 bp (wide, red). The 95% confidence interval for the average lines is shown. **(b)** Scatterplot comparing the relationship between mRNA level and Spo11 oligo signal. The values are in logarithmic scale. The red line shows the linear regression. Correlation score, intercept, and slope are noted. **(c)** Top1-13myc and Top2 binding centered at hotspot summits. Heat maps show all hotspots sorted by level of breakage activity. Average of each quintile is plotted above the heat maps, with the color of the line corresponding to the color beside the heat map quintile. The 95% confidence interval for the average quintile lines is shown. **(d)** Average Spo11-oligo signal in quartiles based on IGR size. Quartile ranges are <294 bp (blue), 294 - 453 bp (green), 454 - 752 bp (red), and >752 bp (black). Signals are centered at IGR midpoints and extended 1kb in each direction. The 95% confidence interval for the average lines is shown. The AUC is quantified in the bar plots above the quartile signal plot. Black bars represent standard error for each quartile. All quartiles are significantly different, except the lowest 2 quartiles ($P < 0.0001$, n.s. P-value = 0.14, Mann-Whitney-Wilcoxon test with Bonferroni correction).



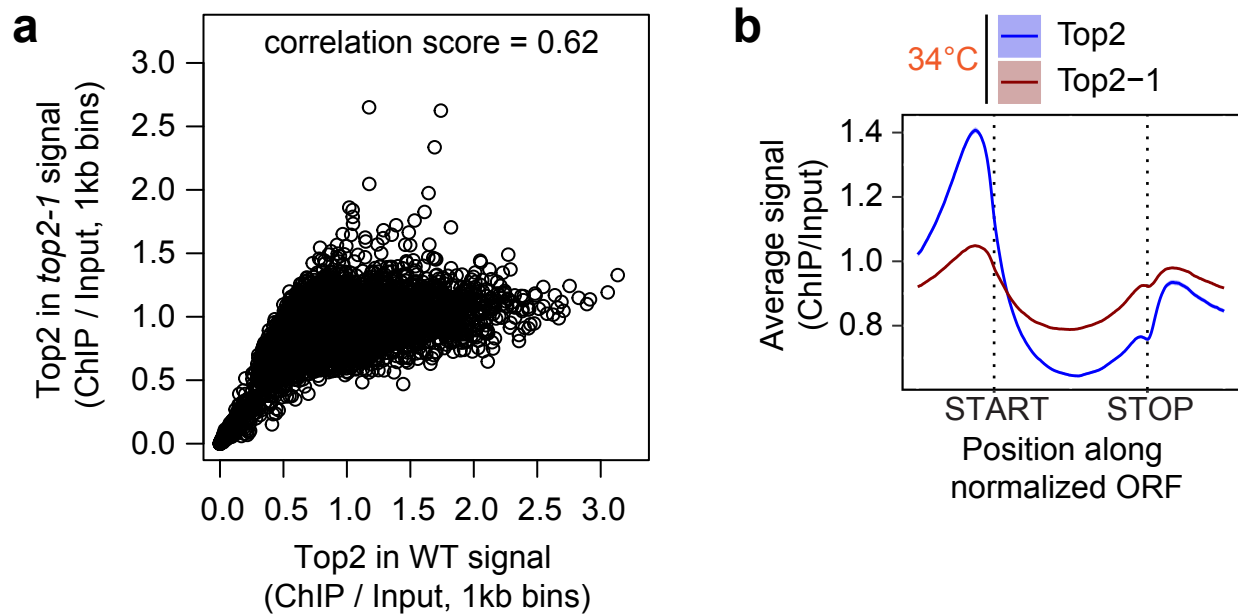
Supplemental Figure 4. SC morphology and sporulation are normal in the absence of Top1.

(a) Immunofluorescence staining for Hop1 and Zip1 on chromosome spreads of wild type and *top1Δ* mutant during meiosis. Scale bars are 5 μm. **(b)** Sporulation efficiency for wild-type and *top1Δ* cells (n=200). **(c)** Spore viability for wild type and *top1Δ* for three experiments (n=88 per experiment). **(d)** Representative images of immunofluorescence staining for Pch2 and Zip1 on wild-type and *top1Δ* chromosome spreads 4-5 hours after meiotic induction. Scale bar is 5 μm.

a**b****c****d**

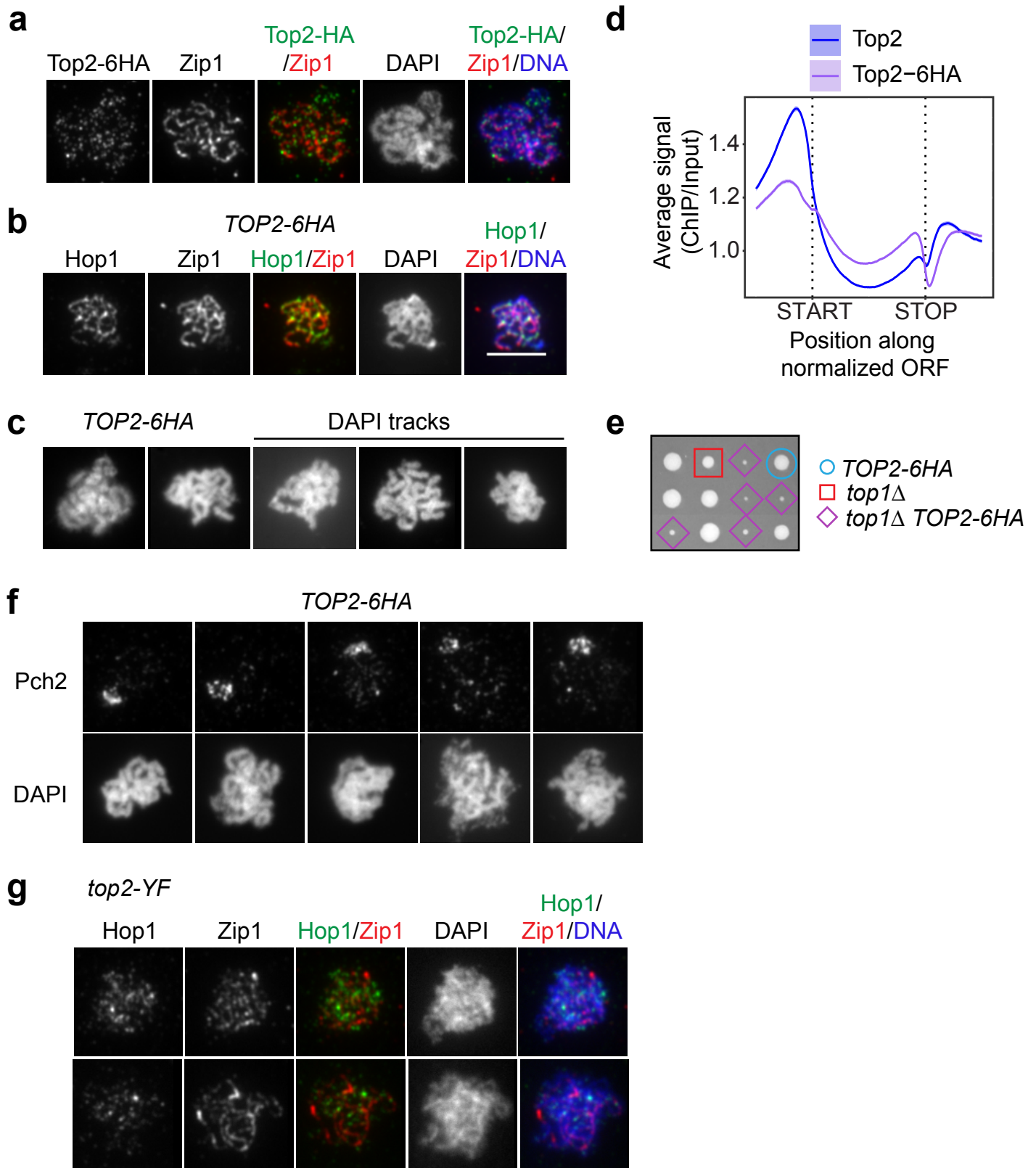
Supplemental Figure 5. Additional analysis of DSB formation in *top2-1*.

Southern blot analysis of the **(a)** *CCT6* and **(b)** *CPA2* hotspots throughout a meiotic time course in *dmc1Δ* and *dmc1Δ top2-1* cells. Cells were shifted to 34°C 1h after meiotic induction. Normalized signal was calculated by subtracting background, dividing the DSB signal by the total signal (parental and DSB bands) and normalizing to the max value of the control. **(c)** Spo11-oligo accumulation in wild-type and *top2-1* cells shifted to restrictive temperature 1 hour after meiotic induction. **(d)** Southern blot analysis of DSBs throughout a meiotic time course across chromosome VIII in *dmc1Δ*, *dmc1Δ spo11Δ*, and *dmc1Δ spo11Δ top2-1* cells. Both panels are taken from the same Southern blot image.



Supplemental Figure 6. Top2 binding is specifically lost in promoters in *top2-1*.

(a) Scatterplot showing the correlation between Top2 and Top2-1 ChIP-seq signal across the genome (correlation = 0.62). **(b)** Metagene analysis of Top2 binding in wild type and the *top2-1* mutants at the restrictive temperature. The 95% confidence interval is shown for the average signals.



Supplemental Figure 7. A C-terminal 6HA tag on Top2 interferes with meiotic chromosome morphogenesis.

(a) Immunofluorescence staining for Top2 and Zip1 on chromosomes spreads of a representative *TOP2-6HA* nucleus. **(b)** Immunofluorescence staining of Hop1 and Zip1 on *TOP2-6HA* chromosomes. **(c)** Representative images of *TOP2-6HA* chromosomes as analyzed by DAPI staining. **(d)** Metagene analysis of *TOP2-6HA* at 30°C. For comparison the profile of Top2 in wild type is shown. The 95% confidence interval is shown for the average signals. **(e)** Three representative tetrads of a *TOP2-6HA* strain crossed with a *top1Δ* strain. Each horizontal quartet of colonies corresponds to a tetrad. Symbols indicate the *TOP2* and *TOP1* genotypes of the respective colonies. **(f)** Example images of diminished chromosomal Pch2 signal on synapsed *TOP2-6HA* chromosomes (as determined by individualized DAPI masses). **(g)** Immunofluorescence staining for Hop1 and Zip1 on chromosome spreads of *top2-YF*. Two representative examples showing wild-type-like distribution of Zip1 and Hop1 (no overlap) are shown. Scale bars are 5 μm.

Supplemental Table 1. Strains used in this study

Strain	Genotype	Background	Used in Figure Panel	Reference
H119	<i>MATa, ho::LYS2, lys2, ura3, leu2::hisG, his4B::LEU2, arg4-Bgl II</i> <i>MATalpha, ho::LYS2, lys2, ura3, leu2::hisG, his4X::LEU2 (Bam)-URA3, arg4-Nsp</i>	SK1	2b, 3b, 5d-h, 6a, 7a-b, S2a-b, S3b	(Bishop et al, 1992)
H7797	<i>MATa, ho::LYS2, lys2, ura3, leu2::hisG, his3::hisG, trp1::hisG</i> <i>MATalpha, ho::LYS2, lys2, URA3, LEU2, HIS3, TRP1</i>	SK1	1a-c, 1e, 1g, 2a, 3a, 3c-d, 4d-i, 6b-c, 7c, S1a-c, S2b, S3a, S3c, S4, S6, S7d	(Subramanian et al, 2016)
H118	<i>MATa, ho::LYS2, lys2, leu2::hisG, his4X::LEU2-URA3, ura3, arg4-nsp, dmc1Δ::ARG4</i> <i>MATalpha, ho::LYS2, lys2, leu2::hisG, his4B::LEU2, ura3, arg4-Bgl2, dmc1Δ::ARG4</i>	SK1	4a-c, 5a-c, S5a-b, S5d	(Bishop et al, 1992)
H8643	<i>MATa, ho::LYS2, lys2, ura3::hisG, leu2::hisG, HIS4, TRP1</i> <i>spo11-Y135F-HA-URA3</i> <i>MATalpha, ho::LYS2, lys2, ura3, LEU2, his3::hisG, trp1::hisG, spo11-Y135F-HA-URA3</i>	SK1	5g	
H10630	<i>MATa, ho::LYS2, lys2, ura3, leu2::hisG, his3::hisG, arg4-Bgl II, spo11-Y135F-HA-URA3, his4B::LEU2, top2-1</i> <i>MATalpha, ho::LYS2, lys2, ura3, leu2::hisG, arg4-Bgl II, spo11-Y135F-HA-URA3, his4B::LEU2, top2-1</i>	SK1	5g	
H9082	<i>MATa, ho::LYS2, lys2, URA3, trp1::hisG, HIS3, , SPO11-6His-3FLAG-loxP-KanMX-loxP</i> <i>MATalpha, ho::LYS2, lys2, ura3, TRP1, HIS3, , SPO11-6His-3FLAG-loxP-KanMX-loxP</i>	SK1	S5c	(Markowitz et al, 2017)
H9012	<i>MATalpha, ho::LYS2, lys2, ura3, leu2, his4B::LEU2, arg4-Bgl II, cyh2-z, SPO11-6His-3FLAG-loxP-KanMX-loxP, top2-1</i> <i>MATa, ho::LYS2, lys2, ura3, leu2, his4X::LEU2-(Bam)-URA3, arg4, cyh2-z, SPO11-6His-3FLAG-loxP-KanMX-loxP, top2-1</i>	SK1	S5c	

H7606	<i>MATa, ho::LYS2, lys2, ura3, leu2::hisG, his4B::LEU2, arg4-Bgl II, top2-1</i> <i>MATalpha, ho::LYS2, lys2, ura3, leu2::hisG, his4X::LEU2-(Bam)-URA3, arg4-Nsp, top2-1</i>	SK1	5d-h, 6, 7a-c, 7c, S6	
H8784	<i>MATalpha, ho::LYS2, lys2, ura3, leu2::hisG, his4B::LEU2, arg4-Bgl II, dmc1Δ::ARG4, top2-1</i> <i>MATa, ho::LYS2, lys2, ura3, leu2::hisG, his4X::LEU2-(Bam)-URA3, arg4-Nsp, dmc1Δ::ARG4, top2-1</i>	SK1	5a-c, S5a-b	
H9847	<i>MATa, ho::LYS2, lys2, ura3, leu2::hisG, his3::hisG, trp1::hisG, TOP1-13Myc::TRP1</i> <i>MATalpha, ho::LYS2, lys2, ura3, leu2::hisG, TRP, arg4, TOP1-13Myc::TRP1</i>	SK1	1a-b, 1d, 1f, 2a, 3d, S1a, S1c-d, S2a, S3c	
H7652	<i>MATalpha, ho::LYS2, lys2, ura3, leu2::hisG, his4X::LEU2-(Bam)-URA3, arg4-Nsp, top1Δ::kanMX6</i> <i>MATa, ho::LYS2, lys2, ura3, leu2::hisG, his4B::LEU2, arg4-Bgl II, top1Δ::kanMX6</i>	SK1	4d-i, S4	
H7833	<i>MATa, ho::LYS2, lys2, leu2::hisG, his4X::LEU2-URA3, ura3, arg4-nsp, dmc1Δ::ARG4, top1Δ::kanMX6</i> <i>MATalpha, ho::LYS2, lys2, trp1, leu2::hisG, his4B::LEU2, ura3, arg4, dmc1Δ::ARG4, top1Δ::kanMX6</i>	SK1	4a-c	
H2817	<i>MATa, ho::LYS2, lys2, ura3, leu2::hisG, his4X::LEU2-(Bam)-URA3, arg4-Nsp, pch2Δ::KanMX4</i> <i>MATalpha, ho::LYS2, lys2, ura3, leu2::hisG, his3::hisG, his4B::LEU2, arg4-Bgl II, pch2Δ::KanMX4</i>	SK1	7c	
H5184	<i>MATa, ho::LYS2, lys2, LEU2, ura3, trp1::hisG, his3::hisG, spo11::TRP1</i> <i>MATalpha, ho::LYS2, lys2, leu2::hisG, URA3, trp1::hisG, HIS+, spo11::TRP1</i>	SK1	3a	
H5187	<i>MATa, ho::LYS2, lys2, his3::hisG, URA, leu2::hisG, TRP, rec8::HIS3MX6</i> <i>MATalpha, ho::LYS2, lys2, his3::hisG, ura3, LEU2, trp1::hisG, rec8::HIS3MX6</i>	SK1	3a	
H9173	<i>MATa, ho::LYS2, lys2, ura3, leu2::hisG, his4B::LEU2, arg4-Bgl II, dmc1Δ::ARG4, spo11Δ::URA3</i> <i>MATalpha, ho::LYS2, lys2, ura3, leu2::hisG, his4B::LEU2, arg4-Bgl II, dmc1Δ::ARG4, spo11Δ::URA3</i>	SK1	S5d	

H9171	<i>MATa, ho::LYS2, lys2, ura3, leu2::hisG, his4B::LEU2, arg4-Bgl II, dmc1Δ::ARG4, top2-1, spo11Δ::URA3</i> <i>MATalpha, ho::LYS2, lys2, ura3, leu2::hisG, his4B::LEU2, arg4-Bgl II, dmc1Δ::ARG4, top2-1, spo11Δ::URA3</i>	SK1	S5d	
H7688	<i>MATalpha, ho::LYS2, lys2, ura3, leu2::hisG, his4X::LEU2-(Bam)-URA3, arg4-Nsp, TOP2-6HA::kanMX6</i> <i>MATa, ho::LYS2, lys2, ura3, leu2::hisG, his4B::LEU2, arg4-Bgl II, TOP2-6HA::kanMX6</i>	SK1	S7a-d, S7f	
H7648	<i>MATalpha, ho::LYS2, lys2, ura3, leu2::hisG, his3::hisG, trp1::hisG, top1Δ::kanMX6</i>	SK1	S7e	
H7653	<i>MATa, ho::LYS2, lys2, ura3, leu2::hisG, his3::hisG, trp1::hisG, TOP2-6HA::kanMX6</i>	SK1	S7e	
H10641	<i>MATa, ho::LYS2, lys2, leu2::hisG, arg4-Nsp, ura3::Top2(Y782F)::URA3, pCLB2-TOP2::KanMX</i> <i>MATalpha, ho::LYS2, lys2, leu2::hisG, his4X::LEU2-(Bam)-URA3, arg4-Nsp, ura3::Top2(Y782F)::URA3, pCLB2-TOP2::KanMX</i>	SK1	S7g	
H8644	<i>MATa, his3Δ1, LEU, LYS, ura3Δ0, RME1(ins-308a), TAO3(E1493Q), MKT1(D30G)</i> <i>MATalpha, HIS3, leu2Δ0, lys2Δ0, URA3, RME1(ins-308a), TAO3(E1493Q), MKT1(D30G)</i>	S288C	3a, S3a	(Vale-Silva et al, 2019)